ENCLOSURE 5

MHI Non-Proprietary Document

L5-04GA585, Analytical Evaluations for Operational Assessment

(Non-Proprietary)

San Onofre Nuclear Generating Station, Unit 2 & 3
REPLACEMENT STEAM GENERATORS

Analytical Evaluations for Operational Assessment

Supplier Status Stamp

VPL No: SO23-617-1-M1543	Rev No: 0	QC: N/A
☐ DESIGN DOCUMENT ORDER NO. 800873488		
☒ REFERENCE DOCUMENT–INFORMATION ONLY ☐ VIRP IOM MANUAL		
MFG MAY PROCEED: ☐ YES ☐ NO ☒ N/A		
STATUS - A status is required for design documents and is optional for reference documents. Drawings are reviewed and approved for arrangements and conformance to specification only. Approval does not relieve the submitter from the responsibility of adequacy and suitability of design, materials, and/or equipment represented. ☐ 1. APPROVED ☐ 2. APPROVED EXCEPT AS NOTED - Make changes and resubmit. ☐ 3. NOT APPROVED - Correct and resubmit for review. NOT for field use.		
APPROVAL: (PRINT / SIGN / DATE) RE: Michael Liu [signature] 5 Oct 2012		
FLS:		
Other:		

SCE DE(123) 5 REV. 3 07/11 REFERENCE: SO123-XXIV-37.8.26

[ ]

Purchase Order No.	4500024051
Specification No.	SO23-617-01R3

CONTENT		REMARKS	PURCHASER	ORDER No.	DATE	Nuclear Plant Component Designing Department Steam Generator Designing Section	
DESCRIPTION	- PAGE			ITEM No.	REFERENCE		
	- SHEET		Edison (MNES)	2591012	[ ]	APPROVED BY	[ ]
TOTAL	85 PAGE			1000		CHECKED BY	
						DESIGNED BY	
						DRAWN BY	—
						—	—
						ISSUE DATE	

Distribution	Edison	PM(S)	COPY	DWG. No.	Rev.No.
	1	1	1	L5-04GA585	2

MITSUBISHI HEAVY INDUSTRIES, LTD.

Revision History

Document No.L5-04GA585

No.	Revision	Date	Approved	Checked	Prepared
0	Initial issue	See cover sheet			
1	-Revised stability ratios and pinning forces due to the change of stabilizer type. -Revised the results of full bundle analyses due to change the input values of manufacturing dispersion.	(			)
2	-Revised in accordance with SCE comments of RSG-SCE/MHI-12-5782.				

Table of Contents

1. Purpose

The purpose of this document is to provide the analytical data to be used for the operational assessment of SONGS Unit-2 RSGs in order to return them to service. Unit-2 A-SG(2E089) is used for the analysis since it was the worst case of Unit RSGs (TTW) but that it will be applied to the operational assessment for all Unit 2 RSGs to return to service. The data are inputs for the probability evaluation of in-plane fluid elastic instability (FEI) of the tubes in the next cycle performed by AREVA (Reference 22). △2

2. Summary

The results of the activities performed by MHI are summarized as follows;

(1) Definitions of 4 Categories and Selection of Representation Tube

Tubes which have AVB wear indications are categorized into 4 categories and a representative tube for each category is selected as described in Section 5.

(2) Pinning force to Prevent In-Plane FEI

The contact force sufficient to activate the AVB support points for in-plane direction in order to prevent in-plane FEI are evaluated as described in Section 6. △2

(3) Stability Ratio Boundary Map

In order to determine the supporting condition when in-plane FEI occur, the stability ratios (SR) of all tubes at various supporting conditions are calculated and the boundary maps are prepared as described in Section 7.

(4) Full Bundle Analyses

The contact forces at each AVB support point of all tubes are calculated by using a complete FEM model of the tube bundle to judge whether each AVB support is active or not as described in Section 8.

3. Methodology of Operational Assessment

Fig.3-1 shows the evaluation flow chart of operational assessment, which is developed by AREVA (Reference 22) through the discussion with MHI. In order to carry out the return to service of SONGS Unit-2, the probability of in-plane FEI shall be less than 5% in the next cycle. The operational power level and operating period of next cycle is determined based on the in-plane FEI probability evaluation.

The tubes which have wear indications are divided into separated categories and a representative tube of each category, which is the tube with the highest in-plane stability ratio in the category, is conservatively selected to evaluate the pinning forces..

For the representative tubes, the pinning forces ample to activate the AVB support points for in-plane direction in order to prevent in-plane FEI are evaluated to be used as criteria to judge whether an AVB support point is active or inactive.

By using a complete model of the tube bundle, the contact forces at tubes-to-AVBs contact points in all tubes are calculated. Based on the criteria of contact force of inactive supports, the probabilities of inactive supports are estimated.

The stability ratios (SR) of all tubes at various supporting conditions are calculated to prepare the boundary maps, which are used to determine the supporting conditions when in-plane FEI occur. Based on the probabilities of inactive supports and the stability ratio boundary maps, the probability of in-plane FEI is obtained.

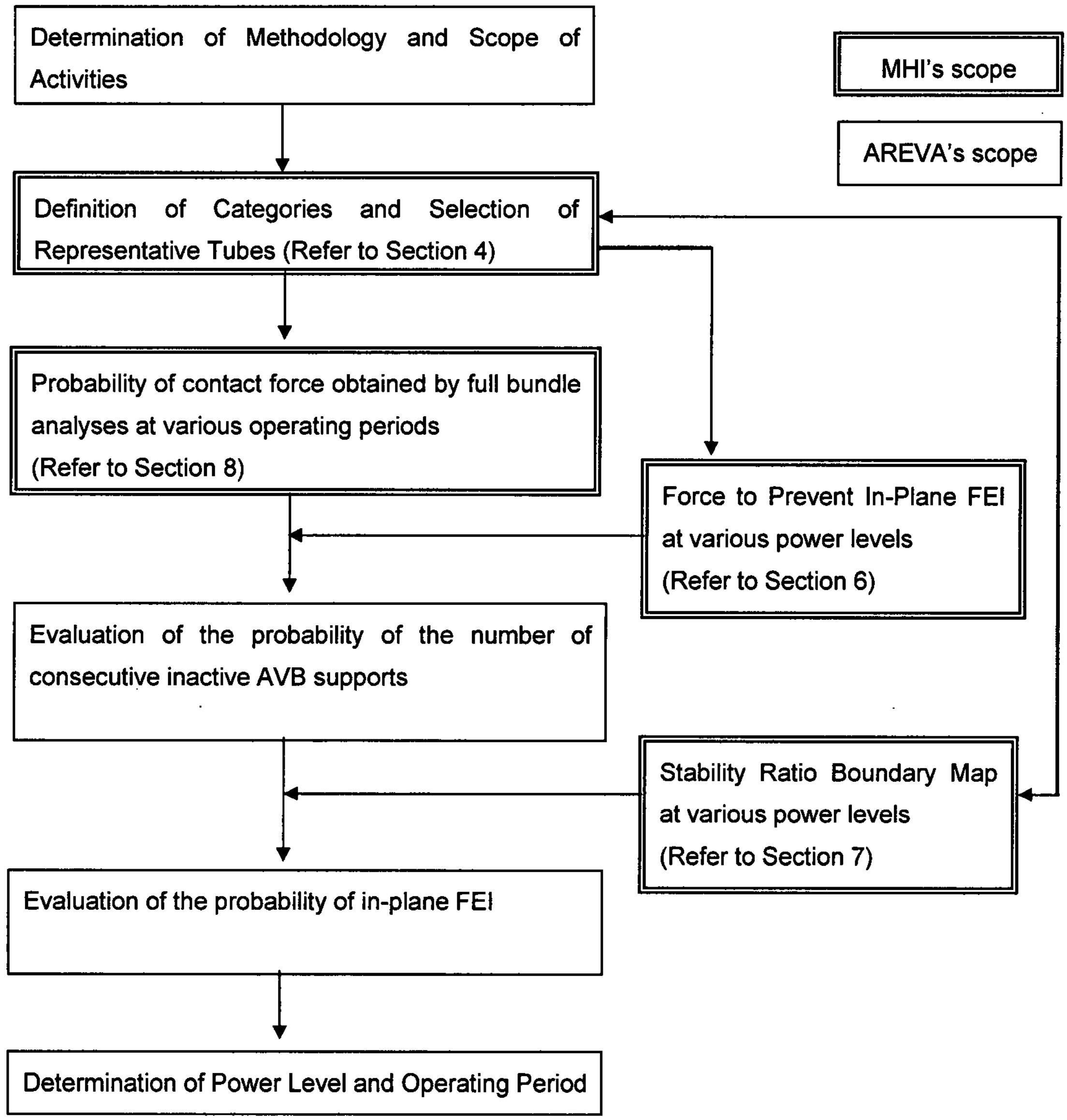

Fig.3-1 Evaluation Flow Chart of Operational Assessment

4. MHI Scope of Supply for Operational Assessment

As shown in Fig.3-1, MHI performed the following activities for the operational assessment as required by AREVA. △2

Definitions of 4 Categories and Selection of Representation Tube	: See Section 5
Force to Prevent In-Plane FEI	: See Section 6
Stability Ratio Boundary Map	: See Section 7
Full Bundle Analyses and Bench Marking Studies	: See Section 8

These results are inputs for the probability evaluation of in-plane fluid elastic instability (FEI) of the tubes in the next cycle performed by AREVA.

5. Definitions of 4 Categories and Selection of Representative Tube

5.1. Definitions of 4 Categories

The tubes of Unit-2A (E089), which have tube-to-tube wear and AVB wear indications, are categorized into 4 categories as follows. The addresses of the 4 categories are shown in Fig.5.1-1.

(1) Plugged tubes which have tube-to-tube wear (TTW) indications: 2 tubes

(2) Plugged tubes which have AVB wear indications: 209 tubes

(3) Unplugged tubes which have AVB wear indications in the center columns (Col.40-138): 554 tubes

(4) Unplugged tubes which have AVB wear indications in the peripheral columns (Col.1-39 and 139-177): 39 tubes

The tubes adjacent to the retainer bars and tubes which have wear indications at only the tube support plate elevations are not taken into consideration.

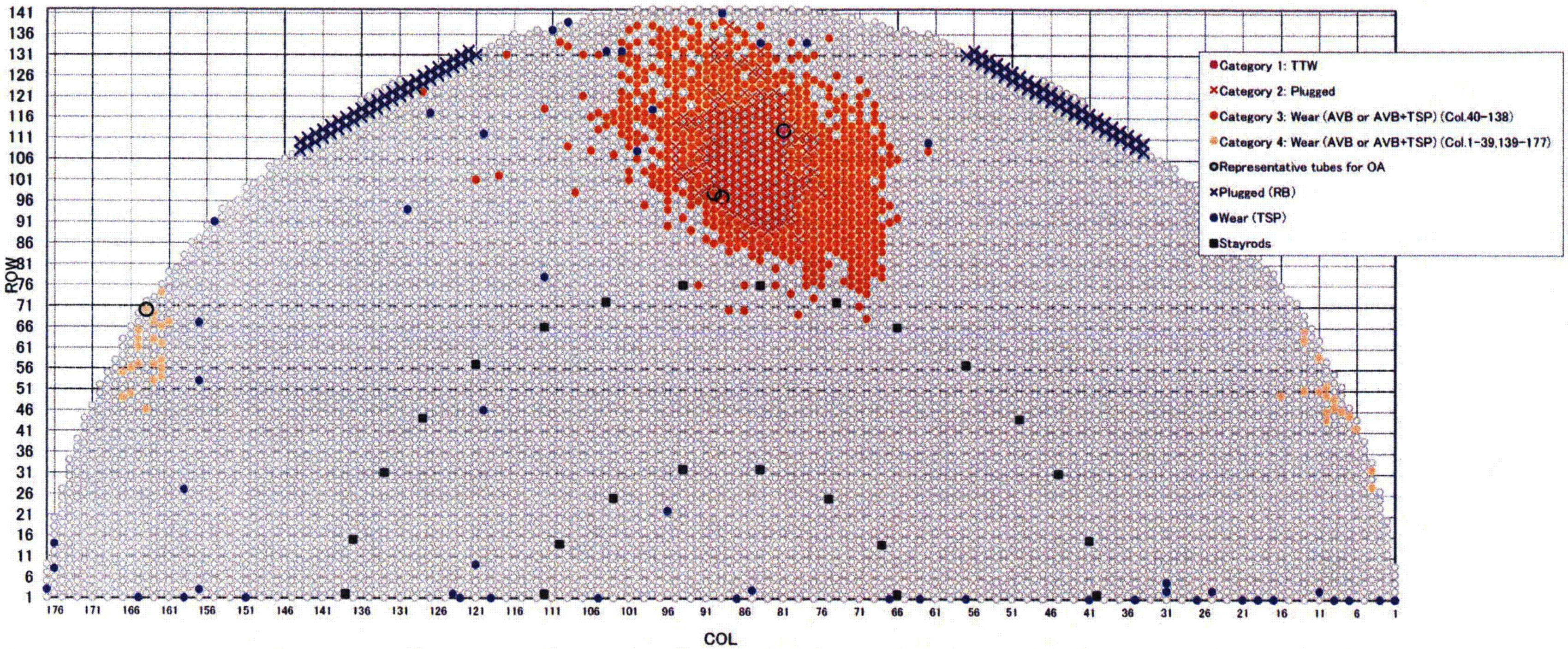

Fig.5.1-1 Definitions of Categories

5.2 Selection of representative tubes

The tubes listed in Table 5.2-1 are selected as representatives, which stability ratios of in-plane FEI with 12 consecutive inactive support points are the maximum in each of the four categories when the thermal power is 70%. Fig.5.2-1 shows the stability ratio map with 12 consecutive inactive support points when the thermal power is 70%. This map is prepared by calculating the stability ratios of 306 representative tubes and the stability ratios of the tubes which were not analyzed were obtained by interpolation method (See Section 7 for detail). A tube map of the 306 representative tubes is shown later as Figure 7.1-2. 2

Table 5.2-1 Representative tubes

	Row	Column	Stability Ratio
(1) Plugged tubes with TTW	113	81	[
(2) Plugged tubes with AVB wear	97	89	
(3) Unplugged tubes with AVB wear in center columns	98*	90*	
(4) Unplugged tubes with AVB wear in peripheral columns	70	164	]

Note *)

*The stability ratios of the tubes which are not analyzed are assumed by interpolation method. Therefore, there is a possibility that a tube with an interpolated stability ratio value in the critical region may have a higher stability ratio than the selected representative tube because interpolated value always calculated lower than the analyzed value. In order to address this inconsistency, a detailed analysis for each tube in the critical region is performed to find out the stability ratio of each tube. From the analysis result, we found out that the tube in Row 96 Column 90 has a slightly (2.2%) higher stability ratio than the tube in Row 98 Column 90, which is the representative tube. However, the impact is very small since these 2 tubes are next to each other and the flow condition is almost identical. Therefore, Row 98 Column 90 is evaluated as a representative. As for other representative tubes, the selected tubes for each category have higher stability ratios than the rest of the tubes in the same category. 2 2

Fig.5.2-1 In-plane SR mapping with 12 consecutive inactive support points when the thermal power is 70%

6. Force to Prevent In-plane motion

6.1. Purpose

The purpose of this evaluation is to obtain the contact force ample to activate the AVB support points for in-plane direction in order to prevent in-plane FEI.

6.2. Conclusion

The criteria of the force to prevent the in-plane motion of representative tubes are evaluated as shown in Table 6.2-1 to 6.2.4.

Table 6.2-1 Summary of Required Contact Forces for 60% Thermal Power

Unit: N

Category	Representative tubes	B01	B 02	B 03	B 04	B 05	B 06	B 07	B 08	B 09	B 10	B 11	B 12
1	R113 C81*												
2	R97 C89*												
3	R98 C90												
4	R70 C164	Evaluation is not needed since the stability ratio is less than 1.0 even if all AVB support points are inactive. (See Section 7 for detail)											

Note)*: Plugged with Type J stabilizer (split stabilizer)

Table 6.2-2 Summary of Required Contact Forces for 70% Thermal Power

Unit: N

Category	Representative tubes	B01	B 02	B 03	B 04	B 05	B 06	B 07	B 08	B 09	B 10	B 11	B 12
1	R113 C81*												
2	R97 C89*												
3	R98 C90												
4	R70 C164	Evaluation is not needed since the stability ratio is less than 1.0 even if all AVB support points are inactive. (See Section 7 for detail)											

Note)*: Plugged with Type J stabilizer (split stabilizer)

Table 6.2-3 Summary of Required Contact Forces for 80% Thermal Power

Unit: N

Category	Representative tubes	B01	B 02	B 03	B 04	B 05	B 06	B 07	B 08	B 09	B 10	B 11	B 12
1	R113 C81*												
2	R97 C89*												
3	R98 C90												
4	R70 C164	Evaluation is not needed since the stability ratio is less than 1.0 even if all AVB support points are inactive.(See Section 7 for detail)											

Note)*: Plugged with Type J stabilizer (split stabilizer)

Table 6.2-4 Summary of Required Contact Forces for 100% Thermal Power

Unit: N

Category	Representative tubes	B01	B 02	B 03	B 04	B 05	B 06	B 07	B 08	B 09	B 10	B 11	B 12
1	R113 C81	[											]
2	R97 C89												
3	R98 C90												
4	R70 C164	Evaluation is not needed since the stability ratio is less than 1.0 even if all AVB support points are inactive.(See Section 7 for detail)											

6.3. Assumption

(1) Fluid force

The turbulent excitation force is evaluated and fluid force caused by FEI is not taken into account due to the following reason.

The purpose of this evaluation is to obtain the contact force ample to activate the AVB support points for in-plane direction in order to prevent in-plane motion.

When the friction force due to contact force is smaller than the turbulent excitation force at an AVB support point, a tube can slide in the in-plane direction. In-plane motion could occur when the tube slides at some AVB support points.

However, if the stability ratio (SR), which is calculated by assuming AVB support points where the tube slides are inactive, is less than 1.0, in-plane FEI will not occur.

For example, SR of a tube is smaller than 1.0 when only 2 support points (B11 and B12) are active while the remaining 10 support points (B01 to B10) are inactive.In this case, if the contact forces at B11 and B12 are the same or greater than the force ample to resist against the turbulent force, in-plane FEI will not occur.

(2) Number of inactive support points

The calculation is performed by assuming that one AVB support point is pinned (with spring element) and other AVB support points are free (with gap in the out-of-plane direction) in order;

(i) To obtain a force ample to resist against the turbulent excitation force with a higher value than the actual condition with more than 1 active support point and,

(ii) To simplify the evaluation of the force since there are too many possible combinations of inactive support points for the evaluation that can be taken into account.

(3) Representative tubes

The representative tubes for Category 1 to 3 (R113 C81 for Category 1, R97 C89 for Category 2 and R98 C90 for Category 3) are evaluated.

The stability ratio of R70 C164 (representative of Category 4) is less than 1.0 even if all AVB support points are inactive. Consequently, there is no probability of in-plane motion in Category 4 and no need to evaluate the pinning force for Category 4.

In order to evaluate the sensitivity of the tube location, additional 2 tubes (Row 131 Column 89 and Row 81 Column 89, which are selected by AREVA) are evaluated as shown in Attachement-1.

6.4. Acceptance criteria

There is no acceptance criterion because the purpose of this evaluation is to determine the contact force ample to prevent in-plane motion.

6.5. Design inputs

6.5.1 Geometry

The tube bundle consists of ¾-inch diameter, thermally treated Alloy 690 U-tubes that are arranged in a 1.0-inch equilateral triangular pitch and are supported by the tubesheet, seven tube support plates, and six sets of anti-vibration bars (AVBs). Tube support plates (TSPs) have broached trifoil tube holes. All the contacting support structures above the tubesheet are made of 405 stainless steel. The nominal dimension of tube, TSPs and AVBs are listed in Table 6.5-1.

6.5.2 Thermal and Hydraulic flow of steam generator secondary side

The ATHOS thermal hydraulic analysis program was used to determine the distributions of fluid gap velocity in the normal direction to tube in-plane and fluid density as the inputs for vibration analysis (See Reference 1 for detail). Fig 6.5-1, Fig.6.5-2, Fig.6.5-3 and Fig.6.5-4 show the flow characteristics at 60%, 70%, 80% and 100% thermal power those are applied to the tubes for the evaluation.

6.5.3 Damping ratio

The damping ratio used for this evaluation is obtained by the same calculation as specified in Reference 1.

Table 6.5-1 Nominal dimensions of tubes, TSPs, and AVBs

Part	Item	Value
Tubes	Material	Thermally treated SB-163 UNS N06690
	Outside diameter	0.75 in
	Thickness	0.043 in
	Number of tubes	9727
	Tube pitch	1.0 in
	Tube arrangement	Triangular
TSPs	Material	[
	Thickness	
	Number of TSPs	
	Tube support span (between TSP centers)	
	Tube support span (from tubesheet to TSP-1)	
AVBs	Material	
	Type	
	Thickness	
	Width	]

(a) Flow Velocity (b) Flow density

Row113 Col81

(a) Flow Velocity (b) Flow density

Row97 Col89

(a) Flow Velocity (b) Flow density

Row98 Col90

Fig. 6.5-1 Flow Characteristics at 60% Thermal Power

(a) Flow Velocity (b) Flow density

Row113 Col81

(a) Flow Velocity (b) Flow density

Row97 Col89

(a) Flow Velocity (b) Flow density

Row98 Col90

Fig. 6.5-2 Flow Characteristics at 70% Thermal Power

[ ]

(a) Flow Velocity (b) Flow density

Row113 Col81

[ ]

(a) Flow Velocity (b) Flow density

Row97 Col89

[ ]

(a) Flow Velocity (b) Flow density

Row98 Col90

Fig. 6.5-3 Flow Characteristics at 80% Thermal Power

[ ]

(a) Flow Velocity (b) Flow density

Row113 Col81

[ ]

(a) Flow Velocity (b) Flow density

Row97 Col89

[ ]

(a) Flow Velocity (b) Flow density

Row98 Col90

Fig. 6.5-4 Flow Characteristics at 100% Thermal Power

6.6. Methodology

All TSP points are modeled to be pinned and the selected AVB support is modeled as the spring element to obtain the reaction force at the selected AVB support. As shown in Table 6-1, 12 cases of 11 inactive support points are evaluated for each representative tube. The analysis model when B07 is active is shown in Fig.6.6-1. 2

The contact force needed to activate the AVB support function in-plane is calculated as follows.

(1) The reaction forces of tube subjected to random excitation (Reaction force of in-plane F_i and out-of-plane F_o) are calculated

$$F_i = \max\left\{\sqrt{F_x(t)^2 + F_z(t)^2}\right\}$$

$$F_o = \max\{F_y(t)\}$$

(2)The contact force F_c, which is sufficient to prevent slip motion by friction force is calculated as follows.

$$F_c = F_i / \mu$$

Where,

μ : Friction coefficient

(3)By taking into account of contact force reduced by the reaction force F_o in the out-of-plane direction, the required contact force, F_{req}, is derived by the equation below.

$$F_{req} = F_c + F_o$$

This methodology is considered to be conservative since the maximum values both of in-plane and out-of-plane are summed. In order to evaluate the sensitivity of changing the evaluation method to calculate the double of standard deviation, the case study is performed as described in Attachment -2.

Table 6.6-1 Active/Inactive Support Points

Evaluated point	B01	B 02	B 03	B 04	B 05	B 06	B 07	B 08	B 09	B 10	B 11	B 12
B01	A	I	I	I	I	I	I	I	I	I	I	I
B02	I	A	I	I	I	I	I	I	I	I	I	I
B03	I	I	A	I	I	I	I	I	I	I	I	I
B04	I	I	I	A	I	I	I	I	I	I	I	I
B05	I	I	I	I	A	I	I	I	I	I	I	I
B06	I	I	I	I	I	A	I	I	I	I	I	I
B07	I	I	I	I	I	I	A	I	I	I	I	I
B08	I	I	I	I	I	I	I	A	I	I	I	I
B09	I	I	I	I	I	I	I	I	A	I	I	I
B10	I	I	I	I	I	I	I	I	I	A	I	I
B11	I	I	I	I	I	I	I	I	I	I	A	I
B12	I	I	I	I	I	I	I	I	I	I	I	A

A: Active support point

I: Inactive support point

[ ]

Fig 6.6.1 Analysis model when B07 is active

6.7 Results

The calculated contact forces are rounded up to be integral numbers as shown below.

6.7.1 60% Thermal Power

The analysis results at 60% thermal power are shown in Table 6.7.1-1 to 6.7.1-3.

Table 6.7.1-1 Required contact force of R113 C81 (with Type J stabilizer)

Unit:N

Evaluated point	B01	B 02	B 03	B 04	B 05	B 06	B 07	B 08	B 09	B 10	B 11	B 12
B01												
B02												
B03												
B04												
B05												
B06												
B07												
B08												
B09												
B10												
B11												
B12												

I: Inactive support point

Table 6.7.1-2 Required contact force of R97 C89 (with Type J stabilizer)

Unit:N

Evaluated point	B01	B 02	B 03	B 04	B 05	B 06	B 07	B 08	B 09	B 10	B 11	B 12
B01												
B02												
B03												
B04												
B05												
B06												
B07												
B08												
B09												
B10												
B11												
B12												

I: Inactive support point

Table 6.7.1-3 Required contact force of R98 C90

Unit:N

Evaluated point	B01	B 02	B 03	B 04	B 05	B 06	B 07	B 08	B 09	B 10	B 11	B 12
B01												
B02												
B03												
B04												
B05												
B06												
B07												
B08												
B09												
B10												
B11												
B12												

I: Inactive support point

6.7.2 70% Thermal Power

The analysis results at 70% thermal power are shown in Table 6.7.2-1 to 6.7.2-3.

Table 6.7.2-1 Required contact force of R113 C81 (with Type J stabilizer)

Unit:N

Evaluated point	B01	B 02	B 03	B 04	B 05	B 06	B 07	B 08	B 09	B 10	B 11	B 12
B01												
B02												
B03												
B04												
B05												
B06												
B07												
B08												
B09												
B10												
B11												
B12												

I: Inactive support point

Table 6.7.2-2 Required contact force of R97 C89 (with Type J stabilizer)

Unit:N

Evaluated point	B01	B 02	B 03	B 04	B 05	B 06	B 07	B 08	B 09	B 10	B 11	B 12
B01												
B02												
B03												
B04												
B05												
B06												
B07												
B08												
B09												
B10												
B11												
B12												

I: Inactive support point

Table 6.7.2-3 Required contact force of R98 C90

2

Unit:N

Evaluated point	B01	B 02	B 03	B 04	B 05	B 06	B 07	B 08	B 09	B 10	B 11	B 12
B01												
B02												
B03												
B04												
B05												
B06												
B07												
B08												
B09												
B10												
B11												
B12												

I: Inactive support point

6.7.3 80% Thermal Power

The analysis results at 80% thermal power are shown in Table 6.7.3-1 to 6.7.3-3.

Table 6.7.3-1 Required contact force of R113 C81 (with Type J stabilizer)

Unit:N

Evaluated point	B01	B 02	B 03	B 04	B 05	B 06	B 07	B 08	B 09	B 10	B 11	B 12
B01												
B02												
B03												
B04												
B05												
B06												
B07												
B08												
B09												
B10												
B11												
B12												

I: Inactive support point

Table 6.7.3-2 Required contact force of R97 C89 (with Type J stabilizer)

Unit:N

Evaluated point	B01	B 02	B 03	B 04	B 05	B 06	B 07	B 08	B 09	B 10	B 11	B 12
B01												
B02												
B03												
B04												
B05												
B06												
B07												
B08												
B09												
B10												
B11												
B12												

I: Inactive support point

Table 6.7.3-3 Required contact force of R98 C90

Unit:N

Evaluated point	B01	B 02	B 03	B 04	B 05	B 06	B 07	B 08	B 09	B 10	B 11	B 12
B01												
B02												
B03												
B04												
B05												
B06												
B07												
B08												
B09												
B10												
B11												
B12												

I: Inactive support point

6.7.4 100% Thermal Power (with no plugging)

The analysis results at 100% thermal power (with no plugging) are shown in Table 6.7.4-1 to 6.7.4-3.

Table 6.7.4-1 Required contact force of R113 C81 △2

Unit:N

Evaluated point	B01	B 02	B 03	B 04	B 05	B 06	B 07	B 08	B 09	B 10	B 11	B 12
B01												
B02												
B03												
B04												
B05												
B06												
B07												
B08												
B09												
B10												
B11												
B12												

I: Inactive support point

Table 6.7.4-2 Required contact force of R97 C89 △2

Unit:N

Evaluated point	B01	B 02	B 03	B 04	B 05	B 06	B 07	B 08	B 09	B 10	B 11	B 12
B01												
B02												
B03												
B04												
B05												
B06												
B07												
B08												
B09												
B10												
B11												
B12												

I: Inactive support point

Table 6.7.4-3 Required contact force of R98 C90

Unit:N

Evaluated point	B01	B 02	B 03	B 04	B 05	B 06	B 07	B 08	B 09	B 10	B 11	B 12
B01												
B02												
B03												
B04												
B05												
B06												
B07												
B08												
B09												
B10												
B11												
B12												

I: Inactive support point

7. Stability Ratio Boundary Map

7.1. Methodology of Preparing Stability Ratio Boundary Map

The methodology of calculating the stability ratios against in-plane FEI is described in Reference 1. As shown in Fig.7.1-1, 9422 tubes are not to be plugged, 211 tubes are to be plugged with the type J stabilizers (0.5" OD, split stabilizer), 15 tubes are to be plugged with the standard stabilizers and 79 tubes are to be plugged without stabilizers for Cycle 17 operation of Unit-2A (E089) SG. Based on the stability ratio calculation results of the representative tubes, the stability ratios of all tube are obtained by the interpolating method as follows.

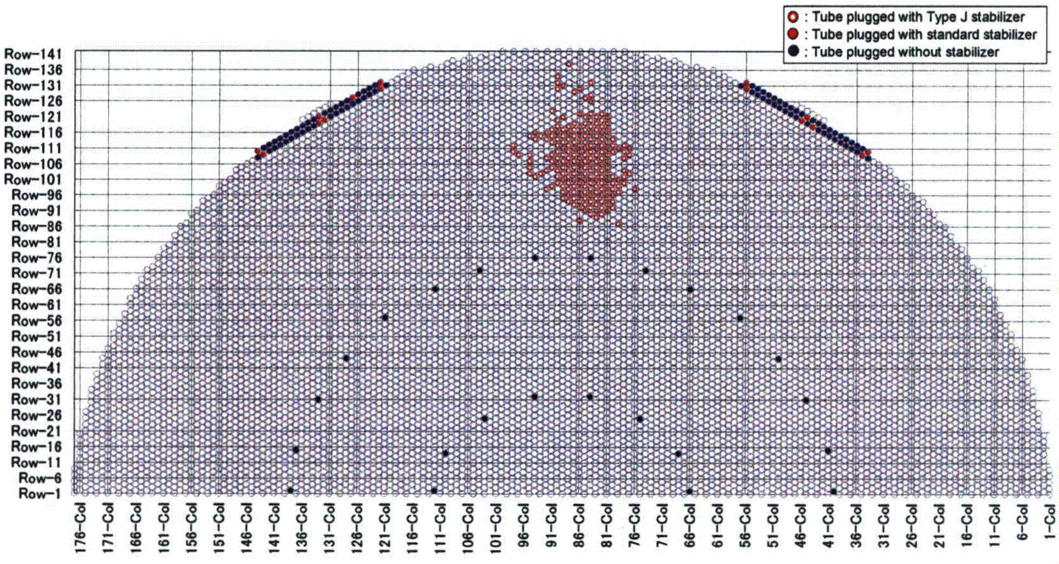

Fig.7.1-1 Plugged Tubes

(1) Unplugged tubes

In order to prepare the maps, the stability ratios are calculated for the representative [ ] tubes as shown in Fig.7.1-2, which are selected for every 4 rows and 4 columns in the outer row region and for every 8 rows and 8 columns in the remaining region. The stability ratios of tubes which are not analyzed are assumed by interpolation method to obtain the stability ratios of all tubes (9727 tubes). For 100% thermal power condition, all tubes are assumed to be unplugged to simulate the stability ratios in Cycle 16.

[ ]

Fig.7.1-2 Representative 306 Tubes to obtain SRs of all tubes

(2) Plugged tubes

For the cases of 60%, 70% and 80% thermal power conditions, the stability ratio of plugged tubes are obtained as follows.

Plugged tubes with Type J stabilizers (split stabilizer)

The stability ratios for 211 plugged tubes in Category-2 are also calculated by interpolating stability ratios of representative tubes. As shown in Fig.7.1-3, the stability ratios of [ ] representative tubes are calculated by assuming all of these [ ] tubes are plugged to obtain the stability ratios of 211 plugged tubes with Type J stabilizer (split stabilizer) by the interpolating method.

[ ]

Fig.7.1-3 Representative 155 Tubes to obtain SRs of plugged tubes

Plugged tubes with standard stabilizers and without stabilizers

The stability ratios of plugged tubes with standard stabilizers and plugged tubes without stabilizers are estimated based on the calculated stability ratios of unplugged tubes by taking into account of the effect of the additional mass of the stabilizer and the decrease of primary coolant mass on the natural frequency and damping as shown in the following equations.

$$f' = \sqrt{\frac{m_0}{m_0'}} \cdot f$$

$$m_0' = m_v + m_s + m_t$$

$$m_0 = m_v + m_p + m_t$$

Where,

f	: Natural frequency of unplugged tube
f'	: Natural frequency of plugged tube
m_0	: Average mass per unit length of unplugged tube
m_0'	: Average mass per unit length of plugged tube
m_v	: Virtual added mass per unit length
m_t	: Mass of tube metal per unit length
m_s	: Mass of stabilizer per unit length*
m_p	: Mass of primary coolant in tube per unit length

Note *) for plugged tube without stabilizer, the additional mass of stabilizer is not taken into account.
As described in Reference 1, the effect of void fraction on the squeeze film damping is not taken into account since plugged tube has no heat transfer.

7.2. AVB Support Conditions

The stability ratios at various supporting conditions are calculated to find the limitation of the number of inactive support points when the stability ratios exceed 1.0 for the evaluation of FEI probability. The inactive support points are assumed to be biased in hot side since the stability ratios are higher than other conditions (e.g. symmetrical or concentrated in cold side).

(1) 60% thermal power

The stability ratio boundary maps are not prepared since the stability ratios of all tubes are smaller than 1.0 even if 12 support points are inactive as shown in Fig.7.2-1.
However, the stability ratio data sets of all tubes for 10 to 12 consecutive inactive support conditions are prepared just in case.

(2) 70% thermal power

The stability ratio boundary maps for the following 2 cases are prepared since the stability ratios of all tubes are smaller than 1.0 when 10 support points are inactive as shown in Fig.7.2-2. In addition, the stability ratio data sets of all tubes for 4 to 12 consecutive inactive support conditions are prepared in order to compare with the stability ratios at 100 % thermal conditions.

- 12 support points are inactive
- 11 support points are inactive (B12 is active)

(3) 80% thermal power

The stability ratio boundary maps for the following 4 cases are prepared since the stability ratios of all tubes are smaller than 1.0 when 8 support points are inactive as shown in Fig.7.2-3.
The stability ratio data sets of all tubes for 7 to 12 consecutive inactive support conditions are prepared just in case.

- 12 support points are inactive
- 11 support points are inactive (B12 is active)
- 10 support points are inactive (B11 and B12 are active)
- 9 support points are inactive (B10, B11 and B12 are active)

(4) 100% thermal power (without plugging) 2

The stability ratio boundary maps for the following 8 cases are prepared since the stability ratios of all tubes are smaller than 1.0 when 4 support points are inactive as shown in Fig.7.2-4.

The stability ratio data sets of all tubes for 4 to 12 consecutive inactive support conditions are also prepared.

- 12 support points are inactive
- 11 support points are inactive (B12 is active)
- 10 support points are inactive (B11 and B12 are active)
- 9 support points are inactive (B10, B11 and B12 are active)
- 8 support points are inactive (B9, B10, B11 and B12 are active)
- 7 support points are inactive (B8, B9, B10, B11 and B12 are active)
- 6 support points are inactive (B7, B8, B9, B10, B11 and B12 are active)
- 5 support points are inactive (B6, B7, B8, B9, B10, B11 and B12 are active)
- 4 support points are inactive (B5, B6, B7, B8, B9, B10, B11 and B12 are active)

Non-proprietary Version

Document No.L5-04GA585(2) (38/85)

MITSUBISHI HEAVY INDUSTRIES, LTD.

Fig.7.2-1 Stability ratio distribution at 60% thermal power when all support points are inactive

Fig.7.2-2 Stability ratio distribution at 70% thermal power when 10 support points are inactive (B11 and B12 are active)

Fig.7.2-3 Stability ratio distribution at 80% thermal power when 8 support points are inactive
(B9, B10, B11 and B12 are active) 2

Fig.7.2-4 Stability ratio distribution at 100% thermal power when 4 support points are inactive
(B5, B6, B7, B8, B9, B10, B11 and B12 are active)

7.3. Stability Ratio Boundary Map

As mentioned in Section 7.2, the stability ratio data set of all tubes in each condition is prepared as shown in Table 7.3-1, which are attached with this report.

Based on the stability ratio data, the stability ratio boundary maps are prepared as shown in Fig.7.3-1,7.3-2 for 70 % thermal power, Fig.7.3-3,7.3-4 for 80% thermal power and Fig.7.3-5,7.3-6 for 100% thermal power. The stability ratio boundary map for 60% thermal power condition is not prepared because all stability ratios at 60% thermal power condition are smaller than 1.0 even if all AVB support points are inactive as described in Section 7.2. Fig.7.3-2, 7.3-4 and 7.3-6 show the tubes of each category in addition to the SR boundaries. The color of each plot indicates the minimum number of inactive AVB support points, when the stability ratio is greater than 1.0. The distribution of color plots is not symmetrical because the stability ratios of the plugged tubes, which are distributed asymmetrically, are estimated as mentioned in Sec.7.1. 2

By using the boundary map of the minimum number of inactive support points when the stability ratio is greater than 1.0, the tubes of each category are categorized by multiple groups as shown in Table.7.3-2 for 60 % thermal power, Table.7.3-3 for 70% thermal power, Table 7.3-4 for 80% thermal power and Table 7.3-5 for 100% thermal power. 2

Table 7.3-1 Stability Ratio Data Set of All Tubes

Thermal power	Number of inactive support points	File name
60 %	10 to 12	SR_Q60_12-10_inactive supports_20120905.xls
70 %	4 to 12	SR_Q70_12-4_inactive supports_20120913.xls 2
80 %	7 to 12	SR_Q80_12-7_inactive supports_20120905.xls
100 %	4 to 12	SR_Q100_with no plugging_12-4inactive supports_20120710.xls

Fig.7.3-1 Stability ratio boundary map at 70% thermal power

Fig.7.3-2 Stability ratio boundary map at 70% thermal power and tubes of each category

Fig.7.3-3 Stability ratio boundary map at 80% thermal power 2

Fig.7.3-4 Stability ratio boundary map at 80% thermal power and tubes of each category ⚠2

Fig.7.3-5 Stability ratio boundary map at 100% thermal power

[ ]

Fig.7.3-6 Stability ratio boundary map at 100% thermal power and tubes of each category

Table 7.3-2 Number of tubes in each group categorized by SR Boundary Map at 60% thermal power

Group	Number of Inactive support points	Category 1 R113 C81	Category 2 R97 C89	Category 3 R98 C90	Category 4 R70 C164	Probability of in-plane FEI
1	SR<1 when 12 AVB support points are inactive					
2	SR≥1 when 12 support points are inactive					
Total (SR<1 when 10 AVB support points are inactive)						

Table 7.3-3 Number of tubes in each group categorized by SR Boundary Map at 70% thermal power 2

Group	Number of Inactive support points	Category 1 R113 C81	Category 2 R97 C89	Category 3 R98 C90	Category 4 R70 C164	Probability of in-plane FEI
1	SR<1 when 12 support points are inactive	[				
2	SR≥1 when 12 support points are inactive SR<1 when 11 consecutive support points are inactive					
3	SR≥1 when 11 consecutive support points are inactive SR<1 when 10 consecutive support points are inactive					
4	SR≥1 when 10 consecutive support points are inactive					
Total (SR<1 when 9 AVB support points are inactive)						]

Table 7.3-4 Number of tubes in each group categorized by SR Boundary Map at 80% thermal power 2

Group	Number of Inactive support points	Category 1 R113 C81	Category 2 R97 C89	Category 3 R98 C90	Category 4 R70 C164	Probability of in-plane FEI
1	SR<1 when 12 AVB support points are inactive					
2	SR≥1 when 12 support points are inactive SR<1 when 11 consecutive support points are inactive					
3	SR≥1 when 11 consecutive support points are inactive SR<1 when 10 consecutive support points are inactive					
4	SR≥1 when 10 consecutive support points are inactive SR<1 when 9 consecutive support points are inactive					
5	SR≥1 when 9 consecutive support points are inactive SR<1 when 8 consecutive support points are inactive					
6	SR≥1 when 8 consecutive support points are inactive					
Total (SR<1 when 7 AVB support points are inactive)						

MITSUBISHI HEAVY INDUSTRIES, LTD.

Non-proprietary Version

Document No.L5-04GA585(2) (51/85)

Table 7.3-5 Number of tubes in each group categorized by SR Boundary Map at 100% thermal power (Rev. 2)

Group	Number of Inactive support points	Category 1 R113 C81	Category 2 R97 C89	Category 3 R98 C90	Category 4 R70 C164	Probability of in-plane FEI
1	SR<1 when 12 AVB support points are inactive					
2	SR≥1 when 12 support points are inactive SR<1 when 11 consecutive support points are inactive					
3	SR≥1 when 11 consecutive support points are inactive SR<1 when 10 consecutive support points are inactive					
4	SR≥1 when 10 consecutive support points are inactive SR<1 when 9 consecutive support points are inactive					
5	SR≥1 when 9 consecutive support points are inactive SR<1 when 8 consecutive support points are inactive					
6	SR≥1 when 8 consecutive support points are inactive SR<1 when 7 consecutive support points are inactive					
7	SR≥1 when 7 consecutive support points are inactive SR<1 when 6 consecutive support points are inactive					
8	SR≥1 when 6 consecutive support points are inactive SR<1 when 5 consecutive support points are inactive					
9	SR≥1 when 5 consecutive support points are inactive SR<1 when 4 consecutive support points are inactive					
10	SR≥1 when 4 consecutive support points are inactive					
Total (SR<1 when 4 AVB support points are inactive)						

8. Full Bundle Analyses

8.1. Purpose

The purpose of this section is to provide the full bundle analyses results in the following cases for the operational assessment of Unit-2 at Cycle 17 and benchmarking studies of Unit-2 and Unit-3 at Cycle 16. 2

8.2. Conclusions

The analyses for Unit-2 after additional 6 months are completed for calculation of in-plane FEI occurrence probability, and the analyses for both of Unit-2 and Unit-3 at BOL and cycle 17 are completed for benchmarking.

8.3. Acceptance Criteria

There is no criterion for this calculation.

8.4. Assumption

(1) The manufacturing dispersion of Unit-2 A-SG (E089) represents Unit-2, and Unit-3 A-SG(E089) represents Unit-3.

(2) The dimensional manufacturing tolerances are based on the actual measurement results. The dimensions, which were not measured but checked by the go/no-go, are assumed based on the drawing tolerances and the AVB pressing test results for the calculated contact forces to be consistent with the ECT ding signals (See Appendix-9 of Reference 2 for details).

(3) Hydrodynamic pressure is neglected in this calculation because friction forces due to manufacturing tolerances are much higher than contact forces caused by hydraulic pressure. Therefore, hydraulic pressure hardly displaces the tubes.

(4) Wear rates have no correlation with thermal power levels in this calculation because AVB wear is caused by random vibration and random vibration is supposed to be independent of thermal power level. Consequently, the wear rates at 17 cycle are assumed to be kept to the additional periods operation. And the contact forces are independent of thermal power level in this calculation.

8.5. Methodology

8.5.1 Analysis model

All parts of the U-bend assembly above the #6 TSP (Tubes, AVBs, Retaining bars, Retainer bars and Bridges) are modeled as beam elements(See Appendix-9 of Reference 2 for details).

Figure 8.5.1-1 shows overview of the analysis model. The analysis model used is a symmetrical quarter model (The validity of quarter model is shown in Attachment-4). The contact points between tube to AVB, and tube to TSP are modeled as gap elements, which show spring property in compression. Stayrod is modeled as tube since the effect of this modeling is negligibly small as shown in Attachment-3.

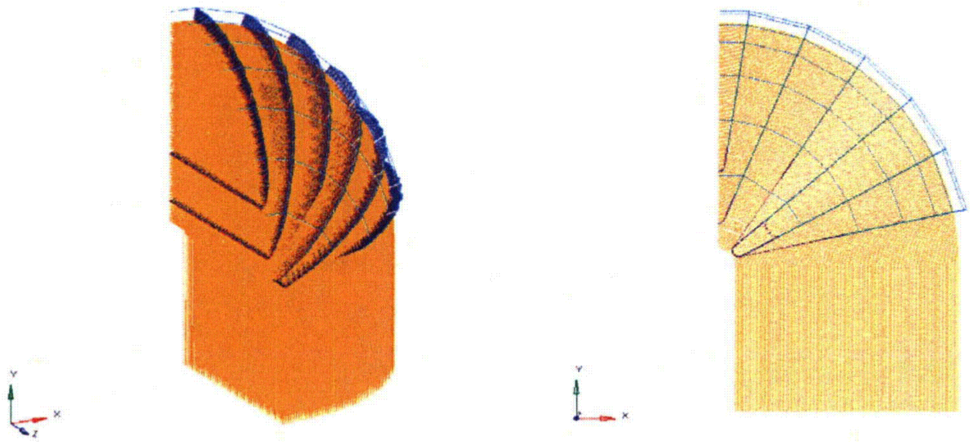

Bird's-eye View of the Model　　　　Front View of the Model

Fig.8.5.1-1 Analysis model

8.5.2 Analysis cases

The analysis cases shown in Tab.8.5.2-1 are performed for the operational assessment of Unit-2 and benchmarking studies for Unit-3.

Table 8.5.2-1 Analysis cases

Cycle	16					17	
Purpose	Bench marking studies					Operational Assessment	
Operation period	Beginning		3 months	12 months	End	6 months	12 months
Condition	Cold	Hot	Hot	Hot	Hot	Hot	Hot
Unit-2 E089	5-9-259	5-9-261 5-9-262 5-9-263 5-9-264	—	5-9-265 5-9-266 5-9-267 5-9-268	5-9-269 5-9-270 5-9-271 5-9-272	5-9-273 5-9-274 5-9-275 5-9-276	5-9-297 5-9-298 5-9-299 5-9-300
Unit-3 E089	5-9-306	5-9-309 5-9-311 5-9-314 5-9-317	5-9-307 5-9-312 5-9-315 5-9-318	—	5-9-308 5-9-313 5-9-316 5-9-319	—	—

2

8.6. Design Inputs

8.6.1 Geometry and manufacturing dispersion

The nominal tube and tube support dimensions are obtained from the design drawings (Reference 3 to 20). The manufacturing dimensional tolerance dispersions of Tube G value, tube pitch, tube flatness, AVB thickness deviation, AVB twist, and AVB flatness are considered in the analysis model. The deviation is generated according to random number and inputted to the gap elements in the analysis model. The random number dispersion follows normal distribution.

Table 8.6.1-1 shows input of manufacturing dispersion to the analysis model.

Table 8.6.1-1 Measurement results of the dimensions

[ ]

8.6.2 Gap distribution and wear depth

(1) Tube wear

The following formula gives the relation between tube wear volume and wear depth at AVB contact point. The relation curve is described in Fig.8.6.2-1.

$$V = \frac{1}{2} R^2 (\phi - \sin\phi) \cdot L$$

$$\phi = \cos^{-1}\left(1 - \frac{h}{R}\right) \times 2$$

V: Wear volume

R: Tube radius

h: Wear depth

L: Wear width

ϕ: Wear angle

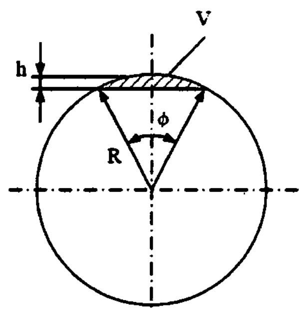

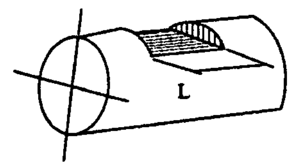

On the other hands, the relation between tube wear volume and wear depth at TSP contact point is expressed as below equation obtained by 3 dimensional model (See Appendix-10 of Reference 2 for detail) and shown in Fig.8.6.2-2.

Fig.8.6.2-1 Tube wear curve at AVB contact point

Fig.8.6.2-2 Tube wear curve at TSP contact point

In this study, tube wear percentage after 22+6 months operation in Unit-2 is predicted according to the following steps with above two curves.

1) Wear percentage after 22 months operation (ECT result) is converted to wear volume.
2) Wear rate is calculated by dividing wear volume by 22 months at each tube contact point.
3) Wear volume after 22+6 months operation is predicted by multiplying wear rate by 22+6 months.
4) Wear percentage after 22+6 months operation is converted from 3) wear volume by using above two wear curves.

The cumulative probabilities of wear percentages at each Category after 22+6 months operation are summarized in Fig.8.6.2-3.

(2) AVB wear

AVB itself is being worn according to tube wear progress. In this study, the condition that AVB wear progresses is taken into account conservatively, because more severe AVB wear makes larger gap between a tube and an AVB.

The ratio of wear coefficient between AVB [ ] and tube (TT690) is estimated to be [ ] based on MHI test results (Reference 21). The test results showed the wear coefficient ratio between [ ] [ ] is [ ] to [ ] Consequently, the wear coefficient ratio [ ] is conservatively regarded as [ ] for this study, which means that AVB wear volume is half of Tube wear volume. In this study, the relation of AVB wear depth with tube wear depth is calculated as follows:

1) To calculate a section of tube wear surface in each tube wear percentage
2) To calculate AVB wear volume by using the ratio of wear coefficient from tube wear volume in each tube wear percentage
3) To calculate AVB wear depth by dividing 2) by 1) in each tube wear percentage

The result of above calculation is shown in Fig.8.6.2-4. Formula of the relation is approximately expressed as [ ] Therefore, AVB wear depth is regarded as [ ] of tube wear depth in this study.

AVB points TSP points

[ ]

Category1: Plugged tubes which have tube-to-tube wear (TTW) indications

AVB points TSP points

[ ]

Category2: Plugged tubes which have AVB wear indications

AVB points TSP points

[ ]

Category3: Unplugged tubes which have AVB wear indications in the center columns (Col.48-130)

AVB points TSP points

[ ]

Category4: Unplugged tubes which have AVB wear indications in the peripheral columns (Col.1-47 and 131-177)

Fig.8.6.2-3 the cumulative probabilities of wear percentages after 22+6 months operation

Fig.8.6.2-4 the relation of wear depth between AVB and tube

8.7. Analysis results

The tube-to-AVB contact forces at all intersections between tubes and AVBs are obtained and the results are included in the electronic files shown in Table 8.7-1, which are attached with this report.

Table 8.7-1 Output Files of Analysis Results

Case	Output File Name
5-9-259	OUTPUT_SONGS_QUARTER_MODEL01_CASE5-9-259_RAND_GAP_STATIC01.dat.csv
5-9-261	OUTPUT_SONGS_QUARTER_MODEL01_CASE5-9-261_RAND_GAP_STATIC01.dat.csv
5-9-262	OUTPUT_SONGS_QUARTER_MODEL01_CASE5-9-262_RAND_GAP_STATIC01.dat.csv
5-9-263	OUTPUT_SONGS_QUARTER_MODEL01_CASE5-9-263_RAND_GAP_STATIC01.dat.csv
5-9-264	OUTPUT_SONGS_QUARTER_MODEL01_CASE5-9-264_RAND_GAP_STATIC01.dat.csv
5-9-265	OUTPUT_SONGS_QUARTER_MODEL01_CASE5-9-265_RAND_GAP_STATIC01.dat.csv
5-9-266	OUTPUT_SONGS_QUARTER_MODEL01_CASE5-9-266_RAND_GAP_STATIC01.dat.csv
5-9-267	OUTPUT_SONGS_QUARTER_MODEL01_CASE5-9-267_RAND_GAP_STATIC01.dat.csv
5-9-268	OUTPUT_SONGS_QUARTER_MODEL01_CASE5-9-268_RAND_GAP_STATIC01.dat.csv
5-9-269	OUTPUT_SONGS_QUARTER_MODEL01_CASE5-9-269_RAND_GAP_STATIC01.dat.csv
5-9-270	OUTPUT_SONGS_QUARTER_MODEL01_CASE5-9-270_RAND_GAP_STATIC01.dat.csv
5-9-271	OUTPUT_SONGS_QUARTER_MODEL01_CASE5-9-271_RAND_GAP_STATIC01.dat.csv
5-9-272	OUTPUT_SONGS_QUARTER_MODEL01_CASE5-9-272_RAND_GAP_STATIC01.dat.csv
5-9-273	OUTPUT_SONGS_QUARTER_MODEL01_CASE5-9-273_RAND_GAP_STATIC01.dat.csv
5-9-274	OUTPUT_SONGS_QUARTER_MODEL01_CASE5-9-274_RAND_GAP_STATIC01.dat.csv
5-9-275	OUTPUT_SONGS_QUARTER_MODEL01_CASE5-9-275_RAND_GAP_STATIC01.dat.csv
5-9-276	OUTPUT_SONGS_QUARTER_MODEL01_CASE5-9-276_RAND_GAP_STATIC01.dat.csv
5-9-297	OUTPUT_SONGS_QUARTER_MODEL01_CASE5-9-297_RAND_GAP_STATIC01.dat.csv
5-9-298	OUTPUT_SONGS_QUARTER_MODEL01_CASE5-9-298_RAND_GAP_STATIC01.dat.csv
5-9-299	OUTPUT_SONGS_QUARTER_MODEL01_CASE5-9-299_RAND_GAP_STATIC01.dat.csv
5-9-300	OUTPUT_SONGS_QUARTER_MODEL01_CASE5-9-300_RAND_GAP_STATIC01.dat.csv
5-9-306	OUTPUT_SONGS_QUARTER_MODEL01_CASE5-9-306_RAND_GAP_STATIC01.dat.csv
5-9-307	OUTPUT_SONGS_QUARTER_MODEL01_CASE5-9-307_RAND_GAP_STATIC01.dat.csv
5-9-308	OUTPUT_SONGS_QUARTER_MODEL01_CASE5-9-308_RAND_GAP_STATIC01.dat.csv
5-9-309	OUTPUT_SONGS_QUARTER_MODEL01_CASE5-9-309_RAND_GAP_STATIC01.dat.csv
5-9-311	OUTPUT_SONGS_QUARTER_MODEL01_CASE5-9-311_RAND_GAP_STATIC01.dat.csv
5-9-312	OUTPUT_SONGS_QUARTER_MODEL01_CASE5-9-312_RAND_GAP_STATIC01.dat.csv
5-9-313	OUTPUT_SONGS_QUARTER_MODEL01_CASE5-9-313_RAND_GAP_STATIC01.dat.csv
5-9-314	OUTPUT_SONGS_QUARTER_MODEL01_CASE5-9-314_RAND_GAP_STATIC01.dat.csv
5-9-315	OUTPUT_SONGS_QUARTER_MODEL01_CASE5-9-315_RAND_GAP_STATIC01.dat.csv
5-9-316	OUTPUT_SONGS_QUARTER_MODEL01_CASE5-9-316_RAND_GAP_STATIC01.dat.csv
5-9-317	OUTPUT_SONGS_QUARTER_MODEL01_CASE5-9-317_RAND_GAP_STATIC01.dat.csv
5-9-318	OUTPUT_SONGS_QUARTER_MODEL01_CASE5-9-318_RAND_GAP_STATIC01.dat.csv
5-9-319	OUTPUT_SONGS_QUARTER_MODEL01_CASE5-9-319_RAND_GAP_STATIC01.dat.csv

2

9. Reference

(1) L5-04GA567 the latest revision, Evaluation of Stability Ratio for Return to Service
(2) L5-04GA564 the latest revision, Tube Wear of Unit-3 RSG – Technical Evaluation Report
(3) L5-04FU001 the latest revision, Component and Outline Drawing 1/3
(4) L5-04FU002 the latest revision, Component and Outline Drawing 2/3
(5) L5-04FU003 the latest revision, Component and Outline Drawing 3/3
(6) L5-04FU021 the latest revision, Tube Sheet and Extension Ring 1/3
(7) L5-04FU022 the latest revision, Tube Sheet and Extension Ring 2/3
(8) L5-04FU023 the latest revision, Tube Sheet and Extension Ring 3/3
(9) L5-04FU051 the latest revision, Tube Bundle 1/3
(10) L5-04FU052 the latest revision, Tube Bundle 2/3
(11) L5-04FU053 the latest revision, Tube Bundle 3/3
(12) L5-04FU111 the latest revision, AVB assembly 1/9
(13) L5-04FU112 the latest revision, AVB assembly 2/9
(14) L5-04FU113 the latest revision, AVB assembly 3/9
(15) L5-04FU114 the latest revision, AVB assembly 4/9
(16) L5-04FU115 the latest revision, AVB assembly 5/9
(17) L5-04FU116 the latest revision, AVB assembly 6/9
(18) L5-04FU117 the latest revision, AVB assembly 7/9
(19) L5-04FU118 the latest revision, AVB assembly 8/9
(20) L5-04FU119 the latest revision, AVB assembly 9/9
(21) WNSY1568 Test results of wear coefficient between TT690 and 405ss
(22) SONGS document 1814-AU651-M0146 (AREVA doc 51-9187230),Operational Assessment, 2

Attachment-1
Case study of Representative Tubes for Evaluation of Force to Prevent In-Plane FEI

1. Purpose

The purpose of this attachment is to evaluate the sensitivity of the forces to prevent the in-plane FEI of additional tubes (R81 C89 and R131 C89) specified by AREVA.

2. Thermal and Hydraulic flow of steam generator secondary side

The ATHOS thermal hydraulic analysis program was used to determine the distributions of fluid gap velocity in the normal direction to tube in-plane and fluid density. Fig A-1 and Fig.A-2 show the flow characteristics of R81 C89 and R131 C89 at 70% and 100% thermal power condition.

(a) Flow Velocity (b) Flow density

Row81 Col89

(a) Flow Velocity (b) Flow density

Row131 Col89

Fig. A-1 Flow Characteristics of R81 C89 and R131 C89 at 70% Thermal Power

(a) Flow Velocity (b) Flow density

Row81 Col89

(a) Flow Velocity (b) Flow density

Row131 Col89

Fig. A-2 Flow Characteristics of R81 C89 and R131 C89 at 100% Thermal Power

3. Results

The difference of contact force between the representative tubes and additional tubes is not significant in both of 70% and 100% thermal power as shown in the following tables.

Table A-1 Summary of Results for 70% Thermal Power

Unit: N

Category	Representative tubes	B01	B 02	B 03	B 04	B 05	B 06	B 07	B 08	B 09	B 10	B 11	B 12
1	R113 C81												
2	R97 C89												
3	R98 C90												
Additional	R81 C89												
Additional	R131 C89												

Table A-2 Summary of Results for 100% Thermal Power

Unit: N

Category	Representative tubes	B01	B 02	B 03	B 04	B 05	B 06	B 07	B 08	B 09	B 10	B 11	B 12
1	R113 C81												
2	R97 C89												
3	R98 C90												
Additional	R81 C89												
Additional	R131 C89												

Attachment-2
Case study of Methodology to Calculate Force to Prevent In-Plane FEI

1. Evaluation Cases

The contact forces required to activate AVB supports can be reduced by changing the evaluation method. Following 2 cases are performed to calculate the contact forces of Row 97 Column 89 (Representative tube of Category 2) at 70% power and 100% power.

Case A (Original case)

The reaction force of in-plane F_i and out-of-plane F_o are calculated as the maximum independently.

$$F_i = \max\left\{\sqrt{F_x(t)^2 + F_z(t)^2}\right\}$$

$$F_o = \max\ \{F_y(t)\}$$

The contact force F_c, which is sufficient to prevent slip motion by friction force is calculated as follows.

$F_c = F_i/\mu$

Where,

μ : Friction coefficient

By taking into account of contact force reduced by the reaction force F_o in the out-of-plane direction, the required contact force, F_{req}, is derived by the equation below.

$F_{req} = F_c + F_o$

Case B (2 σ)

By taking into account of the variability of the turbulent excitation force, 2 σ of the reaction forces of in-plane F_i and out-of-plane F_o are calculated by the following equations.

$$F_i = \sqrt{F_x(t)^2 + F_z(t)^2}$$

$$F_o = F_y(t)$$

$$\sigma = \frac{\sqrt{\frac{1}{N}\sum^{N} F_i^2}}{\mu} + \sqrt{\frac{1}{N}\sum^{N} F_o^2}$$

$$F_{rq} = 2\sigma$$

2. Results

The contact forces of Row 97 Column 89 (Representative tube of Category 2) at 70% power and 100% power are calculated and compared with the original case (Case A) as shown in Table 1-1 and 1-2.

Table 1-1 Contact Force Required to Activate AVB Supports at 70% Thermal Power

Case	Cate gory	Representative tubes	B01	B 02	B 03	B 04	B 05	B 06	B 07	B 08	B 09	B 10	B 11	B 12
A	2	R97 C89	[											]
B	2	R97 C89												

Table 1-2 Contact Force Required to Activate AVB Supports at 100% Thermal Power

Case	Cate gory	Representative tubes	B01	B 02	B 03	B 04	B 05	B 06	B 07	B 08	B 09	B 10	B 11	B 12
A	2	R97 C89	[											]
B	2	R97 C89												

Attachment-3

Influence of a tube at Stay Rod address on Contact forces in the Full Bundle

1. Purpose

There is a tube at the each stay rod address in the full bundle analysis model, although no tube at stay rod address in real full bundle. The stay rod address is shown in Tab.1-1. This attachment provides how much influence the tubes at stay rod addresses have on contact forces between AVBs and tubes in the full bundle.

Tab.1 -1 Stay Rod Address (for the quarter model)

Row	Column	Row	Column	Row	Column
2	40	25	75	57	57
2	66	31	45	66	66
14	68	32	84	72	74
15	41	44	50	76	84

2. Conclusions

Eliminating the tubes at stay rod address decreases contact forces on the adjacent tubes in adjacent column, and increases contact forces on the adjacent tubes in the same column. However, the range of the influence reaches only several tubes, not so large. The cumulative probability of the contact force is almost same between eliminating case and the original case. It can be considered that the full bundle model with a tube at each stay rod address is valid for calculation of the in-plane FEI occurrence probability.

3. Acceptance Criteria

There is no criterion, because this study is just to confirm influence of tube at stay rod address on contact forces between AVBs and tubes.

4. Analysis Case

2 cases are additionally performed in this study. Case 5-2-1 and Case 6-2-1 model a tube at each stay rod address as original case. Case 5-2-5 and Case 6-2-4 model no tube at the stay rod address. Case 5-2-1 and Case 5-2-5 simulate Unit-2 A-SG at Cycle 17th. Case 6-2-1 and Case 6-2-4 simulate Unit-3 A-SG at Cycle 17th.

Tab.4-1 Analysis cases

	Unit	Stay rod address
Case 5-2-1	Unit 2 A-SG	There are tubes at stay rod addresses.
Case 5-2-5	Unit 2 A-SG	There is **no** tube at stay rod address.
Case 6-2-1	Unit 3 A-SG	There are tubes at stay rod addresses.
Case 6-2-4	Unit 3 A-SG	There is **no** tube at stay rod address.

5. Analysis Results

Fig.5-1 shows change of the contact forces between tubes at the same row in Case 5-2-1 and Case 5-2-5. The figures indicate that the contact forces on the adjacent tubes in adjacent column in Case 5-2-5 (with no tube at stay rod address) decrease more than the original case. This is caused by that the 2 AVBs at stay rod address come close due to manufacturing dispersion. Fig. 5-2 shows change of the contact forces between tubes in the same column in Case 5-2-1 and Case 5-2-5. In this comparison, the contact forces in Case 5-2-5 (with no tube at stay rod address) increase more than the original case, since the 2 AVBs at stay rod address come close to each other and the 2 AVBs hold more tightly the adjacent tube in the same column. Same trend of the contact force is confirmed in Fig.5-3 and Fig.5-4 for Unit-3 case. Fig.5-5 and Fig.5-6 give the cumulative probabilities of the contact forces in Category 2+3 in Case 5-2-1 V.S. Case 5-2-5 for Unit 2 A-SG and Case 6-2-1 V.S. Case 6-2-4 for Unit 3 A-SG. The cumulative probabilities are almost same as each other case. Therefore, the full bundle model with a tube at each stay rod address is valid for calculation of the in-plane FEI occurrence probability.

Case5-2-1 (Original Case: with a tube at each stay rod address)

Case5-2-5 (with **no** tube at stay rod address)

Fig.5-1 Contact forces distribution at Row 76 in **Unit 2** (Case 5-2-1 and 5-2-5)

[ ]

Case5-2-1 (Original Case: with a tube at each stay rod address)

[ ]

Case5-2-5 (with **no** tube at stay rod address)

Fig.5-2 Contact forces distribution in Column 84 **in Unit 2** (Case 5-2-1 and 5-2-5)

[ ]

Case6-2-1 (Original Case: with a tube at each stay rod address)

[ ]

Case6-2-4 (with **no** tube at stay rod address)

Fig.5-3 Contact forces distribution at Row 76 in **Unit 3** (Case 6-2-1 and 6-2-4

Case6-2-1 (Original Case: with a tube at each stay rod address)

Case6-2-4 (with **no** tube at stay rod address)

Fig.5-4 Contact forces distribution in Column 84 in **Unit 3** (Case 6-2-1 and 6-2-4)

(a) Case5-2-1 (Original Case: with a tube at each stay rod address)

(b) Case5-2-5 (with **no** tube at stay rod address)

Fig.5-5 Cumulative probabilities of contact force (Category2+3) in **Unit 2** (Case 5-2-1 and 5-2-5)

(a) Case6-2-1 (Original Case: with a tube at each stay rod address)

(b) Case6-2-4 (with **no** tube at stay rod address)

Fig.5-6 Cumulative probabilities of contact force (Category2+3) in **Unit 3** (Case 6-2-1 and 6-2-4)

Attachment-4
Verification of the Quarter Full Bundle Model

1. Purpose
The purpose of this attachment is to verify the quarter full bundle model by comparing the cumulative probabilities of contact forces between the quarter full bundle model and the half full bundle model.

2. Conclusions
The quarter full bundle model is verified because it is confirmed that the results of the quarter model are consistent with the half full bundle model results.

3. Acceptance Criteria
The contact forces in the quarter model are to correspond with the half full bundle model.

4. Assumption
The model area is a quarter by taking into account symmetry, so that the inputted manufacturing dispersion in Hot side is symmetry same as Cold side.

5. Methodology
In order to verify the quarter full bundle model, the following steps are conducted;

1) to input random manufacturing dispersion to the half full bundle model
2) to input the manufacturing dispersion distributed in Hot side of the half full bundle model to the quarter full bundle model
3) to compare of cumulative probability of the contact forces in the quarter full bundle model with the full bundles

6. Verification Results

6.1 Analysis model

All parts of the U-bend assembly above the #6 TSP (Tubes, AVBs, Retaining bars, Retainer bars and Bridges) are modeled as beam elements. Figure 6.1-1 shows overview of the quarter full bundle model. The model area is a quarter by taking into account symmetry. The contact points between tube to AVB, and tube to TSP are modeled as gap elements, which show spring property in compression.

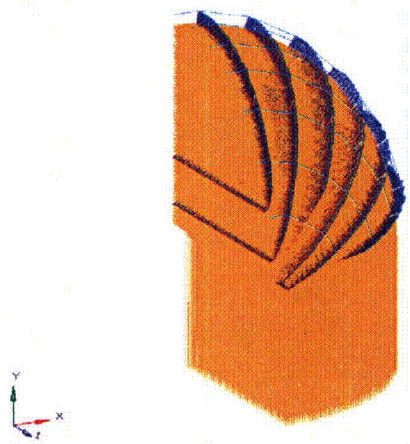
Bird's-eye View of the Model

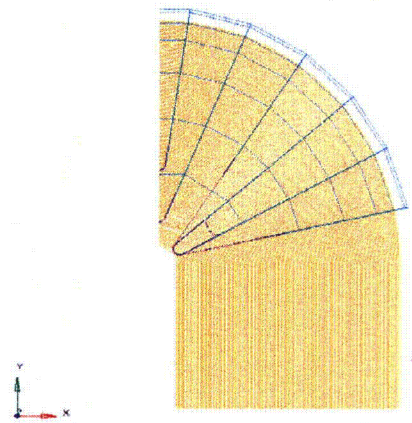
Front View of the Model

Fig.6.1-1 Analysis model

6.2 Analysis cases for verification

The analysis cases for verification are shown in Tab.6.2-1. Random manufacturing dispersions are different between at BOL and after additional 6 months operation.

Tab.6.2-1 Analysis cases for verification

	The quarter model	The half model
Unit-2A at BOL	Case 4-1-106	Case 4-1-98
Unit-2A after additional 6 months operation	Case 4-1-107	Case 4-1-72

6.3 Comparison of cumulative probability of the contact forces

Fig.6.3-1, Fig.6.3-2, Fig.6.3-3, and Fig.6.3-4 show cumulative probabilities of the contact forces on tubes of the quarter model and the half model. The red lines for the quarter good correspond with the blue lines for the half model at from B01 to B05. The probability of lower level contact forces at B6 in the quarter are increased a few more than the half results, because relative displacement between B6 and B7 on a tube is not generated in the quarter model due to symmetry condition, so that there is little off-set loading at B6. However, these differences are judge to be negligible small. Therefore, the quarter full bundle model is valid for the calculation of in-plane FEI occurrence.

Fig.6.3-1 Cumulative probabilities of the contact forces in Category2 of U2A at BOL

[ ]

Fig.6.3-2 Cumulative probabilities of the contact forces in Category3 of U2A at BOL (revision mark 2)

[ ]

Fig.6.3-3 Cumulative probabilities of the contact forces in Category2 of U2A after additional 6 months (2)

[ ]

Fig.6.3-4 Cumulative probabilities of the contact forces in Category3 of U2A after additional 6 months 2